Electrochimica Acta 330 (2020) 135190

Contents lists available at ScienceDirect

Electrochimica Acta

journal homepage: www.elsevier.com/locate/electacta

In situ spectroelectrochemical investigation of a biophotoelectrode based on photoreaction centers embedded in a redox hydrogel

Rafał Białek [a, *], Vincent Friebe [b, c], Adrian Ruff [d], Michael R. Jones [e], Raoul Frese [b], Krzysztof Gibasiewicz [a, **]

[a] Faculty of Physics, Adam Mickiewicz University in Poznań, Ul. Uniwersytetu Poznańskiego 2, 61-614, Poznań, Poland
[b] Department of Physics and Astronomy, LaserLaB Amsterdam, VU University Amsterdam, De Boelelaan 1081, Amsterdam, 1081 HV, the Netherlands
[c] Center for Electrochemical Sciences – Molecular Nanostructures, Faculty of Biochemistry and Chemistry, Ruhr-University Bochum, Universitätsstrasse 150, D-44780, Bochum, Germany
[d] Analytical Chemistry – Center for Electrochemical Sciences (CES), Faculty of Biochemistry and Chemistry, Ruhr-University Bochum, Universitätsstrasse 150, D-44780, Bochum, Germany
[e] School of Biochemistry, Biomedical Sciences Building, University of Bristol, University Walk, Bristol, BS8 1TD, UK

ARTICLE INFO

Article history:
Received 17 June 2019
Received in revised form
31 October 2019
Accepted 31 October 2019
Available online 1 November 2019

Keywords:
Biophotovoltaics
Photobioelectrode
Rhodobacter sphaeroides
Redox hydrogel
Osmium complex
Reaction centers

ABSTRACT

The field of biophotoelectrochemistry and its application in biophotovoltaics and biosensors has gained more and more attention in recent years. Knowledge of the redox potentials of the catalytically active protein cofactors in biophotovoltaic devices is crucial for accurate modelling and in discerning the mechanisms of their operation. Here, for the first time, we used spectroelectrochemical methods to investigate thermodynamic parameters of a biophotoelectrode *in situ*. We determined redox potentials of two elements of the system: the primary electron donor in photosynthetic reaction centers (RCs) of the bacterium *Rhodobacter sphaeroides* and osmium-complex based redox mediators that are bound to a hydrogel matrix. We observe that the midpoint potential of the primary donor is shifted towards more positive potentials in comparison to literature data for RCs solubilized in buffered water solution, likely due to interaction with the polymer matrix. We also demonstrate that the osmium-complex modified redox polymer efficiently wires the RCs to the electrode, maintaining a high Internal Quantum Efficiency with approximately one electron per two photons generated ($IQE = 50 \pm 12\%$). Overall, this biophotoelectrode may be attractive for controlling the redox state of the protein when performing other types of experiments, e.g. time resolved absorption or fluorescence measurements, in order to gain insights into kinetic limitations and thereby help in the rational design of bioelectronic devices.

1. Introduction

With more and more biophotovoltaic device prototypes emerging, determination of the redox potentials of cofactors inside complex proteins is becoming an important topic in the field of bioelectrochemistry. For some small and accessible proteins it is possible to directly measure such potentials via cyclic voltammetry (CV) in solution without additional redox mediators, for example for cytochrome *c* [1]. However, for complex membrane photoproteins such as Photosystem I (PSI) or the *Rhodobacter (Rba.) sphaeroides* Reaction Center (RC) these measurements are challenging due to the typically deeply-embedded nature of the redox centers within the protein scaffold and the surrounding detergent micelle. A direct electron transfer (DET) between the electrode and the protein is thus difficult because of large tunneling distances, and generally necessitate the use of an electron mediator to ensure a mediated electron transfer (MET) regime [2,3]. Electrochemical titration of photosynthetic proteins coupled with spectral measurements has been widely reported in the literature but only for proteins solubilized in solution and in the presence of soluble redox mediators [4–8]. The redox potential of a cofactor buried inside such a protein depends on many factors including the species of organism from which the protein was sourced [6], the type of detergent used for solubilization [7], and the pH or ionic strength of the solution [9,10]. As accurate knowledge of cofactor redox

* Corresponding author.
** Corresponding author.
E-mail addresses: rafal.bialek@amu.edu.pl (R. Białek), krzyszgi@amu.edu.pl (K. Gibasiewicz).

https://doi.org/10.1016/j.electacta.2019.135190

potentials is crucial for the correct description of the mode of operation of bioelectronic devices and for modelling of their performance, there is a need for methodologies for the *in situ* determination of redox potentials in a device setting. At present, it is common practice to rely on literature values obtained for proteins in buffered solutions when discussing or modelling the mechanism of photocurrent or photovoltage generation in a photoelectrochemical device [11,12]. However, such values may not be relevant for a complex photoprotein in a device or on an electrode where the interaction of the protein with the surrounding medium is likely to be different to that in aqueous solution.

The model system we have used to explore solutions to this problem is the RC from the purple bacterium *Rba. Sphaeroides* incorporated in a well-known osmium-complex based redox hydrogel (HG) matrix [13] (Fig. 1A) that was used earlier for the wiring of other photoactive enzymes to the electrode surfaces [14–16]. The RC is a highly-characterized natural solar energy converter that has been used in a variety of both biophotovoltaic [17–19] and biosensing [20] systems, whilst polymer HG with redox active centers such as osmium complexes have been used extensively for the electrochemical wiring of enzymes [21] and other pigment-proteins to electrode surfaces [14,15]. Both systems display redox-dependent absorption change that make them good candidates for a spectroelectrochemical investigation, and have well understood absorbance spectra (Fig. 1C). On deposition of a RC/HG blend on an FTO-glass substrate the osmium-complex species have a potential ($\approx$400 mV vs. SHE) suitable to wire the RC to the electrode for a cathodic current (Fig. 1B), whilst ubiquinone-0 (Q_0) acts as a soluble electron acceptor. The RC comprises of a set of cofactors buried in protein scaffold in two branches (A and B). There are four bacteriochlorophylls, two of which form a dimer that acts as the primary donor of electron (P_{860}) and the other two are accessory bacteriochlorophylls (B_A and B_B). There are also two bacteriopheophytins (H_A and H_B), two quinones (Q_A and Q_B) and one carotenoid (Fig. 1A) [22].

Typically, after light absorption by any of the chromophores in the RC, the energy is transferred to the primary donor forming the P_{860}^* excited state (Fig. 1B). The vast majority of excitation leads to charge separation within 3 ps, forming the $P_{860}^+H_A^-$ state [23]. Later on, the electron is transferred to a quinone at the Q_B binding site, through Q_A, forming the relatively long-lived $P_{860}^+Q_B^-$ state [24]. A current will flow in the cell if wiring of P_{860}^+ and Q_B^- to the electrodes by the osmium HG and Q_0 outcompetes ~1 s lifetime recombination of $P^+Q_B^-$ (Fig. 1B).

Here, we describe the use of a combination of spectroscopic and electrochemical methods for the *in situ* determination of cofactor redox potentials in an assembled biophotovoltaic system with high Internal Quantum Efficiency (50±12 %), characterizing cofactor absorbance and photocurrent as a function of applied potential.

2. Experimental

2.1. Biophotoelectrochemical electrodes

FTO-coated glass slides (TEC 15, Sigma-Aldrich) were cleaned in an ultrasonic bath (Ct-Brand CT-432H1) sequentially in water with 4% TRILUX dish soap solution (Analab), double-distilled water and ethanol for 10 min each. After air-drying a 2-µl drop of aqueous HG-RC blend was placed on the slide surface. Composition of the blend was 5 mg/ml HG, 1 mg/ml wild type RC solution, 0.02 mg/ml poly (ethylene glycol) diglycidyl ether (PEGDGE, acts as crosslinker), 50 mM KCl, 50 mM phosphate buffer pH 7.0. After drop casting, electrodes were incubated in the dark at room temperature overnight. Prior to measurement, electrodes were gently rinsed with double-distilled water to remove loosely bound RCs and HG.

Rba. Sphaeroides RCs were purified as described previously [20].

Osmium-complex based redox HG poly (1-vinylimidazole-*co*-allylamine)-[Os(bpy)$_2$Cl]Cl (with bpy = 2,2′-bipyridine) was synthesized as described previously [13]. Briefly the Os-complex precursor Os(II) (bpy)$_2$Cl$_2$ and the polymer backbone poly (1-vinylimidazole-*co*-allylamine) were refluxed in ethanol in a 1.6:1 mass -ratio for several days. The polymer was precipitated by adding diethyl ether. The crude polymer was purified by several precipitations from ethanol/chloroform solution by adding diethyl ether. The polymer was obtained as a water soluble dark red solid in good yields. The polymer bound Os-complex moieties act as electron relays for shuttling electrons between the electrode surface and the enzyme, while the amino groups in the allylamine co-monomer react with the diepoxy based crosslinker PEGDGE and ensure the formation of stable polymer-enzyme films.

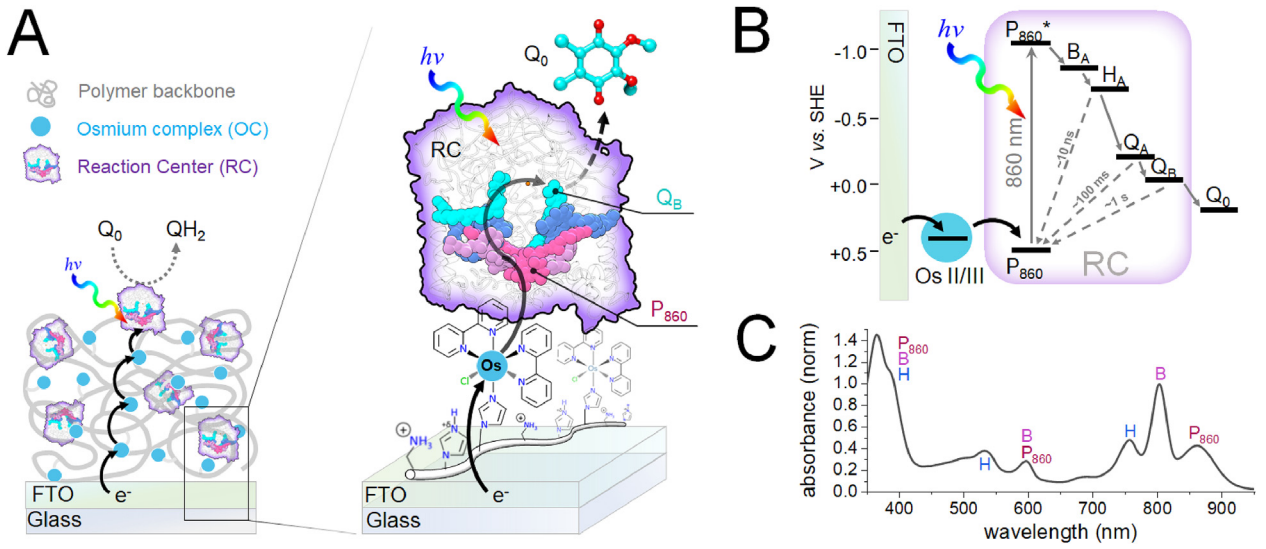

Fig. 1. (A) Scheme of the constructed optically active half-cell. Zoomed picture shows both the chemical structure of the HG and inner structure of RC's cofactors. (B) Energy diagram of the operating half-cell. Additionally, chosen recombination lifetimes inside the RC are presented. (C) Absorption spectrum of the RC solubilized in buffered (20 mM Tris-HCl pH 8.0) solution with detergent (0.1% LDAO).

2.2. Sample characterization

For both photoelectrochemical and absorbance measurements, an FTO-|HG|RC working electrode was employed in a three-electrode configuration in a specially-constructed spectroelectrochemical cell containing an electrolyte of 20 mM citrate buffer (pH 4.0) with 200 mM KCl (and 1.5 mM 2,3-dimethoxy-5-methyl-*p*-benzoquinone (Q_0; Sigma-Aldrich) for photocurrents). Details of the cell design and the experimental setup are given in Supporting Information, Figs. S1–S5. The FTO-|HG|RC working electrode was connected to the potentiostat by copper tape and ports gave access to the working electrode for absorbance measurements or photoexcitation and to the electrolyte for the reference and counter electrodes. For all electrochemical characterizations an Autolab PGSTAT204 potentiostat was used.

For measurements of absorbance change as a function of applied potential a custom setup was built. The measuring UV-VIS-NIR light source was an Avantes combined halogen and deuterium lamp (AvaLight-DH-S-BAL). Broadband detection was achieved using an Avantes HERO (AvaSpec-HSC1024x58TEC-EVO) spectrometer with range 285–1060 nm and 25-μm slit, equipped with a CCD. Light was guided by 600-μm-core optical fibers. The light after exiting the optical fiber before the sample was collimated through a lens (Avantes COL-UV/VIS) and after passing the sample was focused into a second optical fiber through a similar lens and then led to spectrometer. The spectrometer was set to a 200 ms integration time and 20 spectra were averaged for each final spectrum. The light intensity was kept low enough to prevent saturation of the detector in the chosen integration time. Potential was applied in steps lasting 60 s each, as this was enough to reach the plateau in current measurements. Spectra at the plateau of each of these steps were taken for further analysis.

For photocurrent measurements, an 860-nm LED was used whose characteristics are presented in Fig. S6. For each potential, the sample was equilibrated for 120 s prior to illumination, which lasted 30 s. At each potential the photocurrent was determined as the difference between the maximum cathodic current upon illumination and the dark current just before turning on the light.

Measurements of photocurrent External Quantum Efficiency (EQE) spectra were carried out with a photoelectric spectrometer (Instytut Fotonowy). Illumination was via a monochromator from a xenon arc lamp, and light intensity was constantly monitored for correction of the photon flux at the sample. The applied potential was +260 mV vs. SHE. At each wavelength the light was turned on for 10 s and then turned off for 10 s.

2.3. Internal Quantum Efficiency estimation

Internal Quantum Efficiency (IQE) estimation was based on the LED emission spectrum, the RC absorption spectrum in solution and the amplitude of P_{860} absorption band of RCs in HG from spectroelectrochemical measurements (see Supporting Information for details on the calculation). The LED emission spectrum was measured using an Avantes Hero fiber optics spectrometer calibrated for CCD sensitivity. The RC absorption spectrum was measured in buffered (20 mM Tris-HCl pH 8.0) solution with detergent (0.1% LDAO) using a Hitachi U-2800A spectrophotometer.

3. Results and discussion

3.1. Absorption

Absorption spectroscopy at applied potentials between +155 and + 805 mV vs. SHE (Fig. 2A) showed changes in absorbance relative to that at +155 mV vs. SHE attributable to the osmium-complex based redox HG, with maxima around 520 nm and 725 nm, and to the RC in the region between 750 nm and 950 nm. The latter included a highly characteristic bleach at 860 nm and an electrochromic band shift centered at 800 nm.

To confirm these assignments, global analysis with a Nernst curves model was performed on the absorbance data. Global analysis has already proven its utility in the field of time-resolved spectroscopy allowing accurate determination of lifetimes in exponential decay models [25]. The resulting Potential Associated Spectra (PAS) are shown in Fig. 2B (see SI section S3 for details of analysis and the derivation of equations). The PAS associated with a redox midpoint potential (E_m) of +531 ± 6 mV could be attributed to oxidation of the RC P_{860} primary donor, which is well known to cause a bleach at 860 nm and electrochromic blue- and red-shifts centered at 800 nm and 750 nm, respectively, due to the positive charge on P_{860}^{+} [7,8]. The PAS associated with an E_m of +425 ± 3 mV was attributable to the osmium complexes inside the HG matrix, and such shape of spectrum was also observable in a photoelectrode prepared without RCs (Fig. S7).

Fig. 3A shows a full electrochemical titration in which absorbance change (relative to the absorbance at +155 mV) at 520 nm or 860 nm was plotted as a function of time, with the applied potential changed at regular intervals. The data demonstrate that the absorbance changes reporting on the redox state of the RC and the Os-complex based HG were reversible. A plot of absorbance change

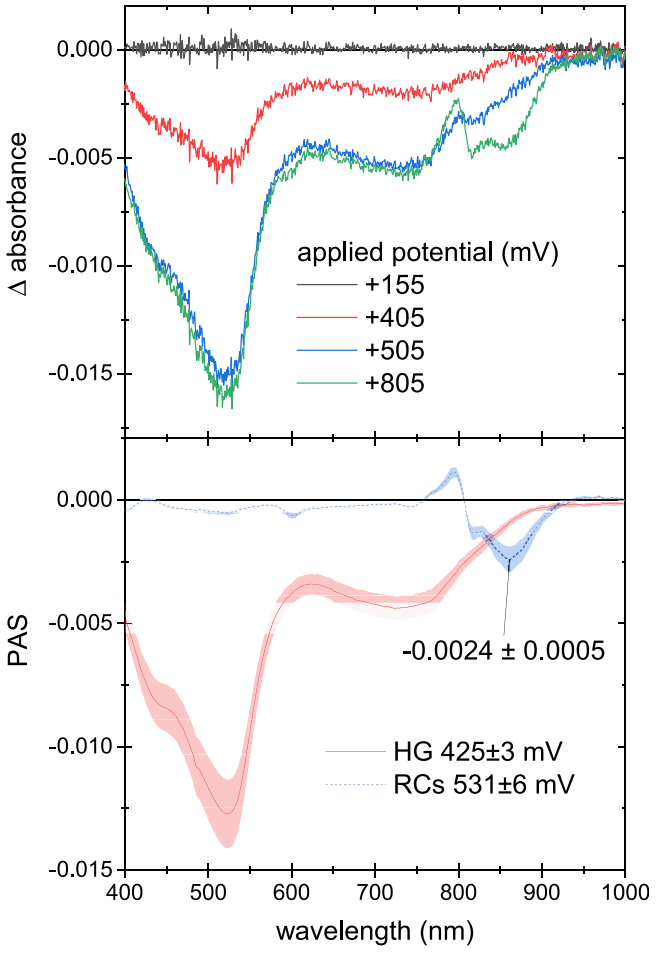

Fig. 2. (A) Absorbance change relative to that at +155 mV of a RC-HG modified FTO-electrode. (B) PAS obtained from global fitting of absorbance change vs. potential measurements. Spectra were averaged between samples (N = 5). Lighter shadow indicates standard deviation.

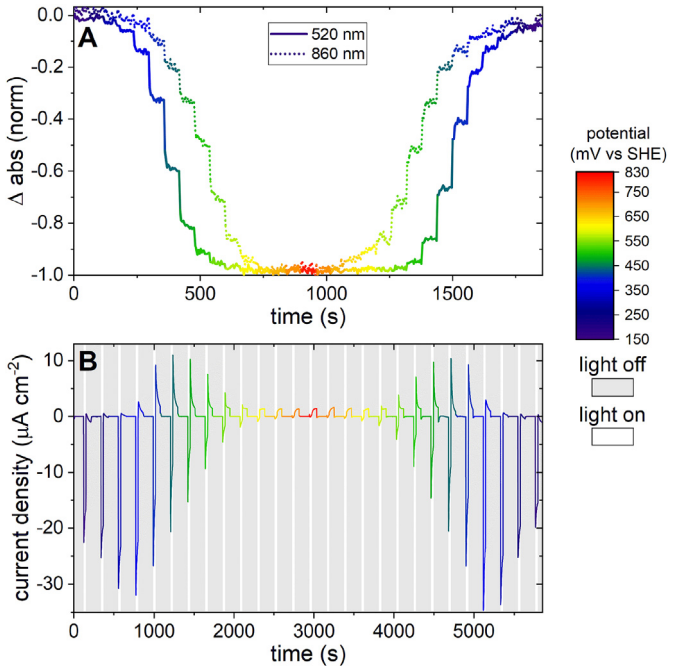

Fig. 3. Time traces for (A) absorbance difference and (B) photocurrent. Data in (A) are normalized for comparison. Data in (B) were corrected for the baseline dark current at each potential.

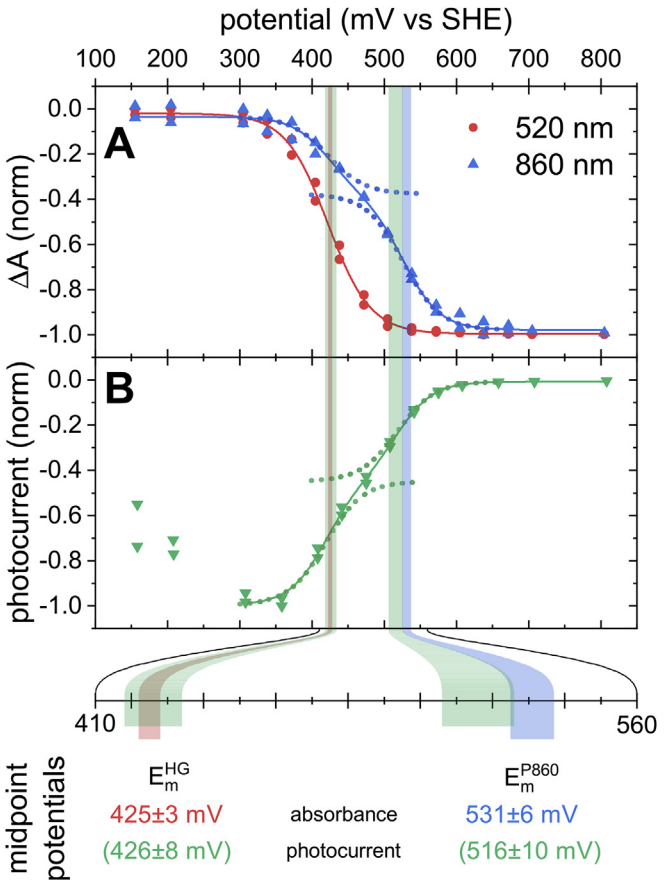

Fig. 4. Electrochemical titration plots for absorption and photocurrents. Vertical bars represent midpoint potentials obtained from color-matching curves with standard deviation. All plots were fitted with either one (red) or two Nernst curves (blue and green). For two-component fits the dotted lines show individual components and the solid line – the sum. (A) Normalized absorbance changes relative to the spectrum at +155 mV. (B) Normalized peak photocurrent. (For interpretation of the references to color in this figure legend, the reader is referred to the Web version of this article.)

at 520 nm as a function of applied potential (Fig. 4A) could be fit with an n = 1 Nernst curve with an E_m at +425 ± 3 mV whilst a plot of the absorbance change at 860 nm was clearly biphasic (Fig. 4A), and could be fit as the sum of two n = 1 Nernst curves with E_m values of 425 ± 3 mV and 531 ± 6 mV.

The amplitude of the PAS attributed to RCs gives the opportunity to determine the amount of electrically connected RCs in the film. The amplitude of the photobleaching band around 860 nm (−0.0024 ± 0.0005) can be attributed to the absorbance of P_{860} in electrically connected RCs in the film in the fully reduced state (without P_{860}^{+} state; see Fig. 1C for comparison). The PAS does not look significantly different to the difference spectrum of P_{860}/P_{860}^{+} presented in literature [7], thus we can estimate the absorbance of the electrically connected RCs at the maximum around 800 nm to be equal to 0.0057 ± 0.0012 based on the absorption spectrum in aqueous solution (Fig. 1C). Using the literature value of the 800 nm extinction coefficient (288 000 $M^{-1}cm^{-1}$) [26] and Lambert-Beer law the surface concentration of the electrically connected RCs was estimated to be Γ_{RCs} = 20±4 $pmol\ cm^{-2}$.

3.2. Photocurrents

Upon illumination by an 860-nm LED (Fig. S6), significant cathodic photocurrents were generated by the RC/osmium-complex polymer working electrode (see example in Fig. S8). The average photocurrent density among different samples (N = 5) at optimal potential and measured with freshly prepared electrode was 52±5 μAcm^{-2}.

A spectrum of photocurrent EQE as a function of excitation wavelength (Fig. 5) was in a good agreement with the absorptance spectrum of the RC confirming it as the source of the photocurrent. We used absorptance spectrum instead of absorption spectrum as the absorptance is proportional to the number of absorbed photons just as photocurrent density is. Variation of the photocurrent density with applied bias potential is shown in Fig. 3B; changes in photocurrent amplitude were again reversible, drop to zero

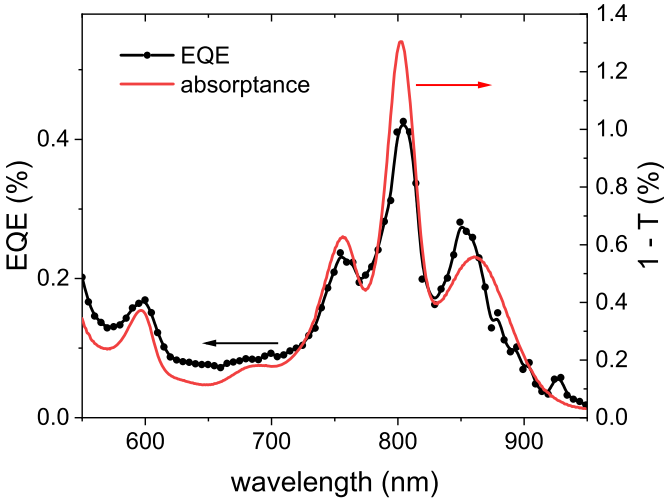

Fig. 5. Photocurrent External Quantum Efficiency (EQE) spectrum of the system compared with the absorptance (1 minus transmission) spectrum taken for RCs in buffered solution (same as in Fig. 1C, but scaled for the thin film absorption).

above +650 mV, and show a maximum around +300 mV. The maximum photocurrent value in Fig. 3B was lower than mentioned above for optimal potential, as the data in Fig. 3B were derived from the second potential sweeping cycle for this sample, thus the sample had undergone partial degradation. After this primary degradation within first potential sweeping cycle the photocurrent and absorbance changes were reversible. Plotting the maximum photocurrent (Fig. 4B), at potentials above +300 mV the decline had a compound sigmoidal shape and could be fitted with the sum of two one-electron Nernst curves with E_m = 426 ± 8 mV and 516 ± 10 mV, in a good agreement with the results from absorbance measurements. Photocurrent vs. potential curve shape is by theory not a simple Nernst curve. However, within the obtained data the fit was sufficient. In general, this shape depends on relative rate constants of electron transfer between different elements of the system and the electrode as well as on electron diffusion constants. However, a full analysis of the latter lies outside the scope of this paper. The lower photocurrents seen at potentials below +300 mV (Figs. 3B and 4B) are likely due to reduction of freely diffusing quinone at the electrode surface, which decreases its ability to receive electrons from RCs (Q_0 is expected to have an E_m of around +230 mV in pH 4.0) [27].

3.3. Internal Quantum Efficiency

IQE of the cells was calculated based on the absorbance amplitude of electrically connected RCs (0.0024 ± 0.0005 at around 860 nm) and photocurrent density (52±5 μAcm^{-2}) to be equal to 50±12 %. It is only 2-fold lower than the quantum efficiency of the charge transfer within RCs in living cells [28]. The high IQE confirms that the investigated system is suitable for deeper characterization as the amount of loss is low. So far lower values of IQE were reported or even not calculated for some systems. One of the highest values so far was IQE of 39% reported for two system in two papers: Friebe et al. [29] for RC-LH1 complexes on rough silver electrodes with plasmon enhancement (white light, 1 sun illumination) and Stieger et al. [30] for PSI on mesoporous ITO (white light, around 1 mW cm^{-2}). Both of these systems consist of porous conductive electrodes and proteins are wired to the surface with cytochrome c. Other system worth mentioning are Langmuir-Blodget (LB) monolayers of RC-LH1 complexes on gold electrodes by Kamran et al. [31] with 32% IQE (880 nm LED, 23 mW cm^{-2}). It shows that even in LB films where the geometry and orientation of proteins is uniform, IQE is lower than in the system with electron mediator filling the space between protein and electrode, such as redox HG. In most of other papers, the IQE reported is below 10% (for example 1.3% for Singh et al. [32]).

3.4. Midpoint potential shift

The E_m^{HG} of redox HG has been reported to depend on pH, ionic strength of the solution and type of protein included in the matrix. In combination with various enzymes and operated under different conditions value for the redox potential of the here used polymer lay in the range from 395 to 463 mV [15,33,34]. Moreover, CV recorded with a HG modifed FTO electrode under the same conditions that are used for the spectroelectrochemical experiments reveal a redox potential for the polymer of 421 mV (see Fig. S9 for sample CV). The value obtained here by absorbance measurements (425 mV ± 3) is in a good agreement with these values, thus confirming the correctness of the method.

The E_m^{P860} of *Rba. Sphaeroides* RCs solubilized in solution has been extensively studied using absorbance measurements coupled with both chemical and electrochemical titration, with values of 450−505 mV reported [7−9,35−42]. The value of 531 mV obtained here by absorbance measurements was at least 25 mV higher than previous reports on RCs in solution, indicating an influence of the Os-complex based hyrogel matrix. It is known that the use of different detergents can cause changes in E_m^{P860} [7], likely due to electric charge and the polarity of surfactant head groups in the vicinity of P_{860}. In the present case the backbone of the redox polymer used to encapsulate the RC as well as the Os-complex based electron mediator are positively charged, which likely shifts E_m^{P860} to the observed higher value. This highlights the importance of the polymer backbone composition in terms of its interaction with the redox active protein.

The obtained difference between E_m^{HG} and E_m^{P860} of about 105 mV gives a driving force lower than that occurring in the natural system with cytochrome c_2 (+300 mV vs. SHE *in vivo*) [43] serving as the electron donor to P_{860}. It may be one of the reasons for lowering of IQE along with unknown spatial coupling of osmium-complex redox centers with RCs. Knowing the exact values of E_m^{HG} and E_m^{P860} *in situ* is a basis for improvement of future designs for example in terms of IQE. On the other hand, a further decrease of the driving force would decrease energy losses in the system, and the net effect of increased voltage of the device and decreased photocurrent (IQE) could be positive.

4. Conclusions

To conclude, although the *Rba. Sphaeroides* RC and related proteins have been used extensively as the basis for a wide variety of bio-photoelectrochemical cells, there has been relatively little attempt to use absorbance spectroscopy to interrogate their properties on an electrode or in a photoelectrochemical cell. In the present work a spectrophotoelectrochemical cell was constructed that enabled measurements of absorbance and photocurrent as a function of applied potential, producing information on the effect of potential on the redox state of key components and their impact on the measured photocurrent. From the EQE spectrum and the differential absorption spectra it was possible to conclude that the RCs remained functionally intact within the HG matrix, and that the midpoint potential of the primary electron donor was shifted towards a more positive potentials than those reported in the literature. Moreover, the IQE of the system was estimated in a relatively high value of 50 ± 12% presenting it as a good model system. This showed the importance of *in situ* measurements when an exact value is necessary for the modelling of mechanism of operation of a biophotovoltaic devices. Looking ahead, a major issue in the design of biophotovoltaic devices is understanding processes such as recombination, electron transfer bottlenecks and energy transfer inefficiencies that limit their photocurrents and photovoltages they can generate. Devices in which absorbance and photocurrent can be measured under controlled redox conditions open the door to the use of time-resolved optical spectroscopy for determination of kinetic rate constants for electron transfer between different parts of the system. Such techniques have unlocked the secrets of the high quantum efficiency of natural solar energy conversion, and there is the prospect of their use to inform iterative rational design of biophotovoltaic devices with improved performance.

Notes

The authors declare no competing financial interests.

Acknowledgment

We would like to thank Prof. Dr. Nicolas Plumeré from Ruhr-University Bochum for fruitful discussions and support in preparation of this work. RB acknowledges support from the Ministry of

Science and Higher Education, Poland (project entitled: "Construction of solar cells based on purple bacteria Reaction Centers and polymer hydrogels" no. 0129/DIA/2016/45). KG acknowledges support from the National Science Center, Poland (project entitled "Bio-semiconductor hybrids for photovoltaic cells" no. 2012/07/B/NZ1/02639). AR thanks the Deutsche Forschungsgemeinschaft (DFG) under Germany's Excellence Strategy EXC-2033 (project number 390677874) for a PostDoc fellowship.

Appendix A. Supplementary data

Supplementary data to this article can be found online at https://doi.org/10.1016/j.electacta.2019.135190.

References

[1] C. Léger, P. Bertrand, Direct electrochemistry of redox enzymes as a tool for mechanistic studies, Chem. Rev. 108 (2008) 2379–2438, https://doi.org/10.1021/cr0680742.
[2] O. Kievit, G.W. Brudvig, Direct electrochemistry of photosystem I, J. Electroanal. Chem. 497 (2001) 139–149, https://doi.org/10.1016/S0022-0728(00)00467-8.
[3] M. Ciobanu, H.A. Kincaid, V. Lo, A.D. Dukes, G. Kane Jennings, D.E. Cliffel, Electrochemistry and photoelectrochemistry of photosystem I adsorbed on hydroxyl-terminated monolayers, J. Electroanal. Chem. 599 (2007) 72–78, https://doi.org/10.1016/j.jelechem.2006.09.019.
[4] A. Nakamura, T. Suzawa, Y. Kato, T. Watanabe, Significant species-dependence of P700 redox potential as verified by spectroelectrochemistry: comparison of spinach and Theromosynechococcus elongatus, FEBS Lett. 579 (2005) 2273–2276, https://doi.org/10.1016/j.febslet.2005.02.076.
[5] A. Nakamura, T. Suzawa, T. Watanabe, Spectroelectrochemical determination of the redox potential of P700 in spinach with an optically transparent thin-layer electrode, Chem. Lett. 33 (2004) 688–689, https://doi.org/10.1246/cl.2004.688.
[6] A. Nakamura, T. Suzawa, Y. Kato, T. Watanabe, Species dependence of the redox potential of the primary electron donor P700 in photosystem I of oxygenic photosynthetic organisms revealed by spectroelectrochemistry, Plant Cell Physiol. 52 (2011) 815–823, https://doi.org/10.1093/pcp/pcr034.
[7] S.S. Deshmukh, H. Akhavein, J.C. Williams, J.P. Allen, L. Kálmán, Light-induced conformational changes in photosynthetic reaction centers: impact of detergents and lipids on the electronic structure of the primary electron donor, Biochemistry 50 (2011) 5249–5262, https://doi.org/10.1021/bi200595z.
[8] S.S. Deshmukh, J.C. Williams, J.P. Allen, L. Kálmán, Light-Induced conformational changes in photosynthetic reaction centers: redox-regulated proton pathway near the dimer, Biochemistry 50 (2011) 3321–3331, https://doi.org/10.1021/bi200169y.
[9] X. Lin, H. a Murchison, V. Nagarajan, W.W. Parson, J.P. Allen, J.C. Williams, Specific alteration of the oxidation potential of the electron donor in reaction centers from Rhodobacter sphaeroides, Proc. Natl. Acad. Sci. U. S. A 91 (1994) 10265–10269, https://doi.org/10.1073/pnas.91.22.10265.
[10] J. Petrović, R.A. Clark, H. Yue, D.H. Waldeck, E.F. Bowden, Impact of surface immobilization and solution ionic strength on the formal potential of immobilized cytochrome c, Langmuir 21 (2005) 6308–6316, https://doi.org/10.1021/la0500373.
[11] R. Białek, D.J.K. Swainsbury, M. Wiesner, M.R. Jones, K. Gibasiewicz, Modelling of the cathodic and anodic photocurrents from Rhodobacter sphaeroides reaction centres immobilized on titanium dioxide, Photosynth. Res. 138 (2018) 103–114, https://doi.org/10.1007/s11120-018-0550-8.
[12] M.T. Robinson, D.E. Cliffel, G.K. Jennings, An electrochemical reaction-diffusion model of the photocatalytic effect of photosystem i multilayer films, J. Phys. Chem. B 122 (2018) 117–125, https://doi.org/10.1021/acs.jpcb.7b10374.
[13] F. Conzuelo, N. Marković, A. Ruff, W. Schuhmann, The open circuit voltage in biofuel cells: nernstian shift in pseudocapacitive electrodes, Angew. Chem. Int. Ed. 57 (2018) 13681–13685, https://doi.org/10.1002/anie.201808450.
[14] T. Kothe, S. Pöller, F. Zhao, P. Fortgang, M. Rögner, W. Schuhmann, N. Plumeré, Engineered electron-transfer chain in photosystem 1 based photocathodes outperforms electron-transfer rates in natural photosynthesis, Chem. Eur J. 20 (2014) 11029–11034, https://doi.org/10.1002/chem.201402585.
[15] T. Kothe, N. Plumeré, A. Badura, M.M. Nowaczyk, D.A. Guschin, M. Rögner, W. Schuhmann, Combination of A Photosystem 1-based photocathode and a photosystem 2-based photoanode to a Z-scheme mimic for biophotovoltaic applications, Angew. Chem. Int. Ed. 52 (2013) 14233–14236, https://doi.org/10.1002/anie.201303671.
[16] K.P. Sokol, D. Mersch, V. Hartmann, J.Z. Zhang, M.M. Nowaczyk, M. Rögner, A. Ruff, W. Schuhmann, N. Plumeré, E. Reisner, Rational wiring of photosystem II to hierarchical indium tin oxide electrodes using redox polymers, Energy Environ. Sci. 9 (2016) 3698–3709, https://doi.org/10.1039/C6EE01363E.
[17] M.R. Jones, The petite purple photosynthetic powerpack, Biochem. Soc. Trans. 37 (2009) 400–407, https://doi.org/10.1042/bst0370400.
[18] V.M. Friebe, R.N. Frese, Photosynthetic reaction center-based bio-photovoltaics, Curr. Opin. Electrochem. 5 (2017) 126–134, https://doi.org/10.1016/j.coelec.2017.08.001.
[19] S.K. Ravi, S.C. Tan, Progress and perspectives in exploiting photosynthetic biomolecules for solar energy harnessing, Energy Environ. Sci. 8 (2015) 2551–2573, https://doi.org/10.1039/C5EE01361E.
[20] D.J.K. Swainsbury, V.M. Friebe, R.N. Frese, M.R. Jones, Evaluation of a biohybrid photoelectrochemical cell employing the purple bacterial reaction centre as a biosensor for herbicides, Biosens. Bioelectron. 58 (2014) 172–178, https://doi.org/10.1016/j.bios.2014.02.050.
[21] A. Ruff, Redox polymers in bioelectrochemistry: common playgrounds and novel concepts, Curr. Opin. Electrochem. 5 (2017) 66–73, https://doi.org/10.1016/j.coelec.2017.06.007.
[22] S.E. D'Haene, L.I. Crouch, M.R. Jones, R.N. Frese, Organization in photosynthetic membranes of purple bacteria in vivo: the role of carotenoids, Biochim. Biophys. Acta Bioenerg. 1837 (2014) 1665–1673, https://doi.org/10.1016/j.bbabio.2014.07.003.
[23] P. Müller, G. Bieser, G. Hartwich, T. Langenbacher, H. Lossau, A. Ogrodnik, M.-E. Michel-Beyerle, The internal conversion rate of the primary donor in reaction centers of Rhodobacter sphaeroides, Berichte Der Bunsengesellschaft Für Phys. Chemie. 100 (1996) 1967–1973, https://doi.org/10.1002/bbpc.19961001207.
[24] J.P. Allen, J.C. Williams, M.S. Graige, M.L. Paddock, A. Labahn, G. Feher, M.Y. Okamura, Free energy dependence of the direct charge recombination from the primary and secondary quinones in reaction centers from Rhodobacter sphaeroides, Photosynth. Res. 55 (1998) 227–233.
[25] I.H.M. van Stokkum, D.S. Larsen, R. van Grondelle, Global and target analysis of time-resolved spectra, Biochim. Biophys. Acta Bioenerg. 1657 (2004) 82–104, https://doi.org/10.1016/j.bbabio.2004.04.011.
[26] S.C. Straley, W.W. Parson, D.C. Mauzerall, R.K. Clayton, Pigment content and molar extinction coefficients of photochemical reaction centers from *Rhodopseudomonas spheroides*, Biochim. Biophys. Acta Bioenerg. 305 (1973) 597–609, https://doi.org/10.1016/0005-2728(73)90079-0.
[27] P. Maróti, C.A. Wraight, The redox midpoint potential of the primary quinone of reaction centers in chromatophores of *Rhodobacter sphaeroides* is pH independent, Eur. Biophys. J. 37 (2008) 1207–1217, https://doi.org/10.1007/s00249-008-0301-4.
[28] C.A. Wraight, R.K. Clayton, The absolute quantum efficiency of bacteriochlorophyll photooxidation in reaction centres of Rhodopseudomonas spheroides, Biochim. Biophys. Acta Bioenerg. 333 (1974) 246–260, https://doi.org/10.1016/0005-2728(74)90009-7.
[29] V.M. Friebe, J.D. Delgado, D.J.K.K. Swainsbury, J.M. Gruber, A. Chanaewa, R. van Grondelle, E. Von Hauff, D. Millo, M.R. Jones, R.N. Frese, Plasmon-enhanced photocurrent of photosynthetic pigment proteins on nanoporous silver, Adv. Funct. Mater. 26 (2016) 285–292, https://doi.org/10.1002/adfm.201504020.
[30] K.R. Stieger, S.C. Feifel, H. Lokstein, M. Hejazi, A. Zouni, F. Lisdat, Biohybrid architectures for efficient light-to-current conversion based on photosystem i within scalable 3D mesoporous electrodes, J. Mater. Chem. A. 4 (2016) 17009–17017, https://doi.org/10.1039/c6ta07141d.
[31] M. Kamran, J.D. Delgado, V. Friebe, T.J. Aartsma, R.N. Frese, Photosynthetic protein complexes as bio-photovoltaic building blocks retaining a high internal quantum E ffi ciency, Biomacromolecules 15 (2014) 2833–2838, https://doi.org/10.1021/bm500585s.
[32] V.K. Singh, S.K. Ravi, J.W. Ho, J.K.C. Wong, M.R. Jones, S.C. Tan, Biohybrid photoprotein-semiconductor cells with deep-lying redox shuttles achieve a 0.7 V photovoltage, Adv. Funct. Mater. 1703689 (2017) 1–8, https://doi.org/10.1002/ADFM.201703689.
[33] A. Badura, D. Guschin, B. Esper, T. Kothe, S. Neugebauer, W. Schuhmann, M. Rögner, Photo-Induced electron transfer between photosystem 2 via cross-linked redox hydrogels, Electroanalysis 20 (2008) 1043–1047, https://doi.org/10.1002/elan.200804191.
[34] F. Zhao, K. Sliozberg, M. Rogner, N. Plumere, W. Schuhmann, The role of hydrophobicity of Os-Complex-Modified polymers for photosystem 1 based photocathodes, J. Electrochem. Soc. 161 (2014) H3035–H3041, https://doi.org/10.1149/2.0081413jes.
[35] D.A. Moss, M. Leonhard, M. Bauscher, W. Mäntele, Electrochemical redox titration of cofactors in the reaction center from Rhodobacter sphaeroides, FEBS Lett. 283 (1991) 33–36, https://doi.org/10.1016/0014-5793(91)80547-G.
[36] J.C. Williams, R.G. Alden, H.A. Murchison, J.M. Peloquin, N.W. Woodbury, J.P. Allen, Effects of mutations near the bacteriochlorophylls in reaction centers from rhodobacter sphaeroides, Biochemistry 31 (1992) 11029–11037, https://doi.org/10.1021/bi00160a012.
[37] H.A. Murchison, R.G. Alden, J.P. Allen, J.M. Peloquin, A.K.W. Taguchi, N.W. Woodbury, J.C. Williams, Mutations designed to modify the environment of the primary electron donor of the reaction center from rhodobacter sphaeroides: phenylalanine to leucine at L167 and histidine to phenylalanine at L168, Biochemistry 32 (1993) 3498–3505, https://doi.org/10.1021/bi00064a038.
[38] V. Nagarajan, W.W. Parson, D. Davis, C.C. Schenck, Kinetics and free energy gaps of electron-transfer reactions in Rhodobacter sphaeroides reaction centers, Biochemistry 32 (1993) 12324–12336, https://doi.org/10.1021/bi00097a008.
[39] K. Artz, J.C. Williams, J.P. Allen, F. Lendzian, J. Rautter, W. Lubitz, G. Feher, Relationship between the oxidation potential and electron spin density of the primary electron donor in reaction centers from Rhodobacter sphaeroides,

Biophys. Approv. 94 (1997) 13582−13587, https://doi.org/10.1073/pnas.94.25.13582.
[40] J.P. Ridge, P.K. Fyfe, K.E. McAuley, M.E. van Brederode, B. Robert, R. van Grondelle, N.W. Isaacs, R.J. Cogdell, M.R. Jones, An examination of how structural changes can affect the rate of electron transfer in a mutated bacterial photoreaction centre, Biochem. J. 351 Pt 3 (2000) 567−578, https://doi.org/10.1042/0264-6021:3510567.
[41] T.N. Kropacheva, A.J. Hoff, Electrochemical oxidation of bacteriochlorophyll a in reaction centers and antenna complexes of photosynthetic bacteria, J. Phys. Chem. B 105 (2001) 5536−5545, https://doi.org/10.1021/jp003381b.
[42] D. Spiedel, M.R. Jones, B. Robert, Tuning of the redox potential of the primary electron donor in reaction centres of purple bacteria: effects of amino acid polarity and position, FEBS Lett. 527 (2002) 171−175, doi:Pii S0014-5793(02)03203-9.
[43] R.C. Prince, P.L. Dutton, The pH dependence of the oxidation-reduction midpoint potential of cytochromes *c*2 in vivo, BBA - Bioenerg 459 (1977) 573−577, https://doi.org/10.1016/0005-2728(77)90055-X.